Excitation of a single atom with a temporaly shaped light pulses

Syed Abdullah Aljunid, Gleb Maslennikov, Yimin Wang,* Dao Hoang Lan,† Valerio Scarani, and Christian Kurtsiefer‡

(Dated: March 22, 2012)

We investigate the interaction between a single atom and optical pulses with a controlled temporal envelope. By switching the temporal shape from rising exponential to square profile, we show that the rising exponential envelope leads to higher excitation probability for a fixed photon number. The atomic transition saturates for ≈ 50 photons in a pulse. Rabi oscillations with 100 MHz frequency are visible in detected fluorescence for excitations powers of ≈ 100 photons in 5 ns pulse.

INTRODUCTION

Quantum networks are viewed as one of the essential developments in quantum information science [**? ? ?**]. In most scenarios, the resource of the quantum network is entanglement that is shared between the network nodes and that is distributed through quantum channels by carriers. Naturally, one can think of atomic two-level systems as nodes, and single photons as carriers. Boosting the efficiency of on-site interactions between photons and atoms and scaling quantum networks to many sites is one of the most pursued tasks in experimental quantum information [**?**].

The exchange of information between atoms and photons is done by fundamental processes of emission and absorption. It is thus highly desirable to achieve an excitation probability of an atom by a photon close to unity. It is common to solve this problem in a context of cavity QED, where the field strength of single photons at the location of the atom is dramatically increased by using optical cavities with small mode volumes [**?**]. However complicated highly reflective dielectric coatings are required to decouple the cavity from environmental losses which compromises the scaling of such system to many node operations. To relax the coating requirements, the mode volume has to be further decreased and several experimental efforts target this issue [**?**], It was also demonstrated that placing an atomic 2-level system at the focus of a simple lens also leads to reasonably strong interaction [**? ? ?**]. In this case, the emission and absorption of photons are not affected by presence of cavities and their efficiency depends on the *overlap* between atomic and photonic spatial and frequency modes. Considering only dipole allowed transitions and lifetime limited spectral absorption profile, it can be shown [**? ?**] that near perfect excitation probability can be achieved with a wavepacket that has an exponentially rising temporal envelope with a characteristic time on the order of the decay time of the excited atomic state. The difference in excitation probability between this pulse and pulses with other envelopes depends on the spatial overlap and expected to be maximal when the spatial distribution of incoming field matches the dipolar pattern of atomic emission [**?**].

In this letter we investigate the effect of temporal shaping of light pulses on the excitation probability of a closed cycling transition in single ^{87}Rb atom.

THEORY

We are interested in determining the excitation probability $\mathrm{P_e}$ of a two-level atom by a travelling light pulse. This probability is given by an expectation value of a Pauli operator $\hat{\sigma}_z = |e\rangle\langle e| - |g\rangle\langle g|$ [**? ? ?**]

$$\mathrm{P_e(t)} = \frac{1}{2}\left(\langle\Psi_0|\hat{\sigma}_z|\Psi_0\rangle + 1\right), \tag{1}$$

where $|\Psi_0\rangle = |g\rangle|\Phi_p\rangle|vac\rangle$ is the initital state of atom+field system. We thus start with atom being in the ground state $|g\rangle$, a field is given by state $|\Phi_p\rangle$ and the environment is initially in the vacuum state $|vac\rangle$. In our experiments, the field is prepared in a coherent state wavepacket

$$|\Phi_p\rangle = \exp\left(\alpha\hat{A}^\dagger - \alpha^*\hat{A}\right)|0\rangle, \tag{2}$$

with average photon number N

$$\mathrm{N} = \langle\Phi_p|\hat{A}^\dagger\hat{A}|\Phi_p\rangle = |\alpha|^2. \tag{3}$$

Here $\hat{A}^\dagger$ is the wavepacket operator that is defined such that when it acts on vacuum, the result is a single photon Fock state wavepacket with spectral distribution function $f(\omega_k)$ and spatial mode function $u_{\mathbf{k},\lambda}(r)$ as in [**?**]

$$\hat{A}^\dagger|0\rangle = \sum_\lambda \int d^3\mathbf{k}\, u^*_{\mathbf{k},\lambda}(r) f(\omega_k)\hat{a}^\dagger_{\mathbf{k},\lambda}|0\rangle = |1\rangle. \tag{4}$$

Upon interaction of such a field with an atom, one gets the expression for the dynamical coupling strength $\mathrm{g(t)}$

$$\mathrm{g(t)} = \sqrt{\Gamma_p\,\mathrm{N}}\,\xi(\mathrm{t}), \tag{5}$$

where

$$\xi(\mathrm{t}) = \frac{1}{\sqrt{2\pi}}\int d\omega\, f(\omega_k)\,\mathrm{e}^{-i(\omega-\omega_0)t} \tag{6}$$

is the Fourier transform of the wavepacket spectral distribution function (temporal envelope) and Γ_p is the decay rate

of the atom into the pulse mode. It is determined by the spatial overlap of the pulse mode with the dipolar emission pattern and for a transition with dipole matrix element d and frequency ω_a, is given by

$$\Gamma_p = \frac{1}{2(2\pi)^2}\left(\frac{\omega_a}{c}\right)^3 \frac{d^2}{\hbar\epsilon_0}\Lambda. \qquad (7)$$

Here $\Lambda = \left[0, \frac{8\pi}{3}\right]$ determines the solid angle subtended by a pulse mode. For $\Lambda = \frac{8\pi}{3}$, $\Gamma_p = \Gamma$ is the total spontaneous emission rate, obtained within Wigner-Weisskopf theory. The excitation probability of equation 1 is obtained by solving a system of coupled differential equations for time-dependent operators [**?**], in which the coupling strength $\mathrm{g(t)}$ enters as a parameter. **Do we show these equations!!??**. Thus, excitation probability of an atom interacting with a coherent light wavepacket depends on a solid angle, subtended by a spatial pulse mode Λ (spatial overlap), temporal bandwidth of the pulse and its shape $\xi(\mathrm{t})$ (frequency-temporal overlap) and number of photons in a pulse N. We assumed that polarization of the pulse was matched to the direction of atomic dipole in equation 7.

In our experiment, the spatial overlap is fixed by a waist of the Gaussian beam $\mathrm{w_L}$ and the focal length of aspheric lens f. In principle, the overlap can be obtained, by measuring the reflection of coherent cw light from a single atom [**? ?**]. Knowing the amount of photons scattered by the atom (from the extinction measurement with APD 1 at Figure) one just detects the amount of clicks in the reflection arm (APD 2) and thus obtains the collection efficiency by dividing the click detection rate by photon scattering rate. In our case, we measured $\approx$ 2.7%. collection efficiency. This fixes our Λ at $0.027 \cdot \frac{8\pi}{3}$.

EXPERIMENTAL SETUP

The experimental setup is schematically shown in Figure 1.

The atom is trapped at the focus of two confocally positioned aspheric lenses in a Far-Off Resonant Optical Dipole Trap (FORT). The FORT is loaded from a magneto-optical trap (MOT) consisting of $\approx 10^4$ atoms. Due to collisional blockade one can achieve a subpoissonian atom distribution with either zero or one atom in a trap at any instance of time [**?**]. The probe beam defines a light mode that is coupled to the atom and is delivered from a single mode optical fiber. This fixes a spatial mode to be Gaussian with a characterstic waist of $\mathrm{w_L} = 1\,mm$ at the focussing lens. If no atom is present in the trap, the second lens recollimates back the probe beam, then it passses through several filters and finally is coupled to another single mode fiber with 72% efficiency (point B to point C on Figure 1). The other end of the fiber is attached to an avalanche photodiode operating in photon counting mode. Atomic fluorescence from MOT beam is collected into a single mode fiber that is coupled to APD2 and gives us a trigger signal, indicating that the atom has loaded into the FORT. After 5 ms of molasses cooling we optically pump the atom to

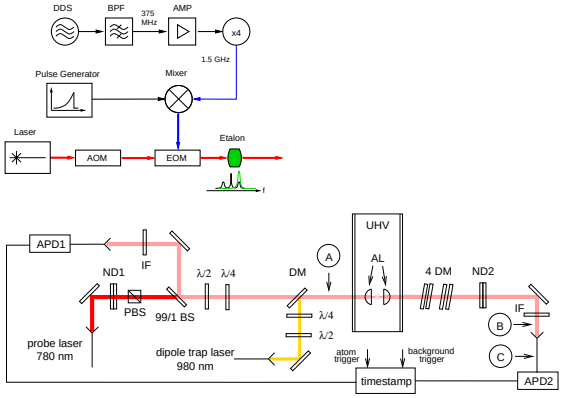

FIG. 1: Top: Setup for preparation of pulses with controllable waveform. DDS: direct digital synthesizer, BPF: stripline filter, AMP: power amplifier. Bottom: Setup for transmission and reflection measurement of light by a single atom. UHV: ultra high vacuum ($< 10^{-11}$ mbar) chamber, AL: aspheric lenses with full NA=0.55 and focal length $\mathrm{f} = 4.51$ mm, PBS: polarizing beam splitter, ND 1,2: stacks of neutral density filters, λ_i's: retardation waveplates, DM: dichroic mirrors, IF: intererence bandpass filters centered at 780 nm, FWHM = 1 nm.

$5\mathrm{S}_{\frac{1}{2}}|\mathrm{F}=2,\mathrm{m_F}=-2\rangle$ with circularly polarized probe light for 10 ms. Then we send a train of 100 optical pulses with varying temporal shape, photon number and characteristic time to the atom. The optical frequency $\mathrm{f_{opt}}$ of the pulse is resonant to $5\mathrm{S}_{\frac{1}{2}}|\mathrm{F}=2,\mathrm{m_F}=-2\rangle \rightarrow 5\mathrm{P}_{\frac{3}{2}}|\mathrm{F}=3,\mathrm{m_F}=-3\rangle$. This value of the frequency is obtained by independent measurement of probe's transmission with cw light. It includes the shift of Zeeman sublevels due to the circularly polarized trap field. The repetition rate of the sequence depends mostly on the dead time of detectors and in our case was 83.3 kHz.

After probing, we check if the atom escapes the trap by shining molasses beams for 20-30 ms. If atom is still inside, the probing sequence is repeated. Once the atom escapes, the same sequence of pulses is recorded for 3 seconds and serves as the reference/background measurement. Since it is possible to use both forward and backward detection directions with respect to the probe propagation, we can study both the transmission and reflection properties of the probe beam by a single atom. Two single photon avalanche photodiodes were used to detect transmitted/reflected light and the temporal histogram of detection events was obtained with a timestamp unit. We triggered the timestamp such that one could process the data differentiating events when the atom was present or absent in the trap. In the following section we describe the pulse preparation and detection scheme in more detail.

Preparation of excitation pulses with tailored temporal envelope

The scheme for generating optical pulses with varying temproal overlap is shown in Figure 1a. The detailed description of its performance is given elsewere [**?**]. In brief, an electrical

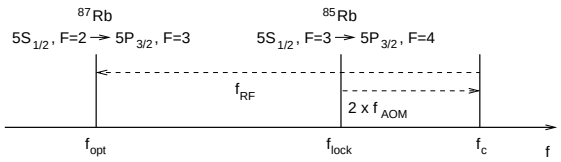

FIG. 2: Evolution of probe laser frequency while passing through modulators.

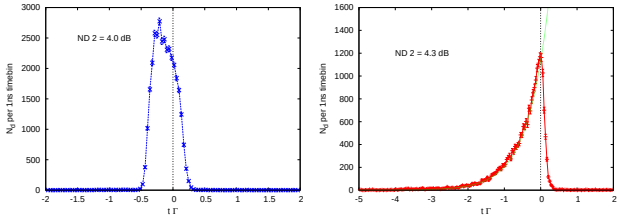

FIG. 3: Rectangular and rising exponential excitation pulses. Histograms show the number of detected events $\mathrm{N_d}$ in 1 ns time bin versus time expressed in units of natural decay rate $\Gamma = 26.3\,\mathrm{ns}$ of $5\mathrm{P}_{\frac{3}{2}}|\mathrm{F}=3\rangle$ in $^{87}\mathrm{Rb}$. (Left) Rectangular shape pulse with temporal width of 15 ns and calculated photon number $\mathrm{N} = 104 \pm 5$. (Right) Rising exponential pulse with characteristic time $\tau = 15\,\mathrm{ns}$ and photon number $\mathrm{N} = 110 \pm 6$. Green line is the fit according to equation 8. The errorbars are due to Poissonian counting statistics.

pulse with a defined envelope is mixed with an RF signal and fed into the fast EOM (20 GHz bandwidth). We used a home-built circuit where we exploited the relation between base voltage and collector current of a fast RF transistor to generate exponential pulses. The electrical pulse can be switched on or off by an external signal in standard logic. We also used the common rectangular envelope which was obtained from a standard NIM pulse from a pattern generator. The probe laser in initially locked to $5\mathrm{S}_{\frac{1}{2}}|\mathrm{F}=3\rangle \rightarrow 5\mathrm{P}_{\frac{3}{2}}|\mathrm{F}=4\rangle$ in ^{85}Rb. The cw probe light is first sent through an acousto optic modulator (AOM) that is used as a primary switch for the optical pulse. The frequency of the probe light is then increased by twice the AOM frequency $\mathrm{f_{AOM}}$ (see Figure 2).

The optical power extinction after the doubly passed AOM is around 50dB. Then, the chopped probe is sent through an EOM where it acquires frequency sidebands which are separated from a carrier frequency $\mathrm{f_c}$ by a frequency of the RF wave $\mathrm{f_{RF}}$. We chose $\mathrm{f_{RF}} = 1.5\,\mathrm{GHz}$ such that the first red sideband frequency is near resonance of the cycling transition $5\mathrm{S}_{\frac{1}{2}}|\mathrm{F}=2\rangle \rightarrow 5\mathrm{P}_{\frac{3}{2}}|\mathrm{F}=3\rangle$ in $^{87}\mathrm{Rb}$. By fine tuning of $\mathrm{f_{AOM}}$ we can find the resonance frequency $\mathrm{f_{opt}}$. In the low modulation regime, the optical power in the first sidebands is almost linear with respect to the RF modulation power. Thus, the modulation temporal envelope is mapped into the sidebands directly. To filter the first red sideband from the carrier we use three consecutive optical resonators with FWHM linewidth of $\approx 460\,\mathrm{MHz}$ that are temperature tuned to transmit the sideband frequency. In the end we achieve ≈ 60 dB attenuation of carrier power. Then the pulses were coupled to single-mode fiber and delivered to the atom.

The number of photons in each pulse was varied by inserting pre-calibrated neutral density filters (ND1 at Figure 1) into the beam. The actual number of photons together with characteristic pulse time was measured by fitting the histogram of the photodetection events.

Photodetection scheme

This histogram was obtained by registering the arrival time of the photodetection events in transmission and reflection arms from two APDs. The APD in the reflection arm is an actively quenched Perkin Elmer single photon counting module with dead time of $\approx 20\,\mathrm{ns}$ and quantum efficiency of 50%. The other APD is a homemade passively quenched diode with a dead time of $\approx 3\,\mu s$ and quantum efficiency of 55%. The timestamp unit is a 4 channel time recorder with two channels used as triggers and two channels receive signals from APD's. The deadtime of the timestamp after each registered event is 120 ns and temporal resolution is $\approx 450\,\mathrm{ps}$. To compensate for the deadtime of the timestamp, a cable delay of 300 ns was added to the APD 1 path. The histogram is obtained by arranging the detection time into bins with temporal widths $\Delta\mathrm{t_b}$ and plotting the probability to find a click in each bin per each trigger pulse.

MEASUREMENT OF PULSE PARAMETERS

In our experiment we investigate interactions of the atom with pulses of two different shapes: rectangular and rising exponential. The envelope shape is defined as

$$\xi_{\mathrm{rect}}(t) = \begin{cases} \sqrt{\Omega} & : \mathrm{for}\, 0 \leq t \leq \frac{1}{\Omega} \\ 0 & : \mathrm{else} \end{cases}$$

for a rectangular pulse and

$$\xi_{\mathrm{exp}}(t) = \begin{cases} \sqrt{\Omega}\exp\left(\frac{\Omega}{2}t\right) & : \mathrm{for}\, 0 \leq t \\ 0 & : \mathrm{for}\, t > 0 \end{cases}$$

for a rising exponential pulse. Here Ω is the frequency bandwidth of the pulse that can be expressed in terms of overall spontaneous emission rate Γ. To extract the photon number and temporal width of excitation pulses, we acquire the histogram of photocounts with no atom in trap in the forward direction with APD 2 see Figure 3.

The photon number is obtained by summing all detected events $\mathrm{N_{d,i}}$ in time bins $\Delta\,\mathrm{t_i}$ per number of triggers $\mathrm{N_T}$ and dividing the obtained number by losses in beam path $\mathrm{N} = \frac{1}{\eta_l \eta_{\mathrm{ND_2}}} \sum_i \frac{\mathrm{N_{d,i}}}{\mathrm{N_T}}$. The losses were measured to be $\eta_l = 0.3 \pm 0.02$ and include quantum efficiency of APD, coupling efficiency to single mode fiber and reflection losses from all optical components. Attenuation due to ND 2 stack of filters is measured to 0.5 % uncertainty and varies from 2.5–5.1 dB.

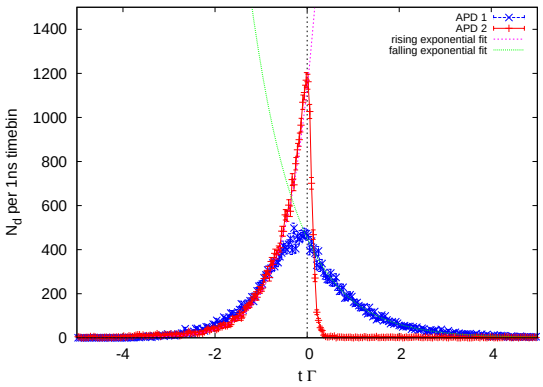

FIG. 4: Histogram of atomic fluorescence photocounts (blue trace) and of excitation pulse (red trace). Initially, when the pulse is ON, the fluorescence rate is determined by coupling to the field in the pulse. When the pulse is finished, the atomic population and thus fluorescence decays exponentially with decay rate Γ. The errorbars are due to Poissonian counting statistics

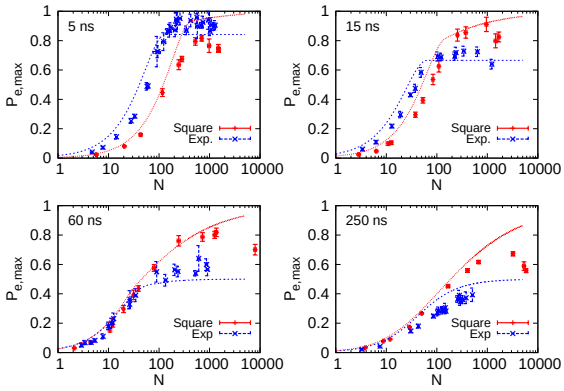

FIG. 5: Maximal excitation probability versus the average photon number in the pulse. Four plots correspond to different temporal banwidths. Theory curves were obtained by numerically solving differential equations for time-dependent operators [**?**].

The bandwidth of rectangular pulse was directly inferred from a histogram and for exponential pulse, we used a following fit function to obtain its characteristic time τ

$$\mathrm{N_{det}(t)} = \eta_l \eta_{\mathrm{ND_2}}\, \mathrm{N} \exp(\frac{\mathrm{t}-\mathrm{t_0}}{\tau}) \times \exp(\frac{\Delta\,\mathrm{t}}{\tau} - 1). \qquad (8)$$

Here the first exponential term reflects the envelope function and the second is due to Poissonian distribution of photocounts. Note that the characterization of the pulses was done immediately after measurement of atomic response, during the background measurement right after atom left the trap. We are thus confident, that pulse parameters did not significantly change during interaction with atom.

RESULTS

We quantify the interaction by measuring the excitation probability of the atom by detecting fluorescent photons in backward direction with APD 1. The temporal evolution of detected photocounts is direcly related to the expectation value of atomic operators and allows us to determine the occupancy of the excited state, that is the excitation probability $\mathrm{P_e}$. In Figure 4 we show the histogram of photocounts obtained by exciting the atom with a rising exponential pulse of Figure 3

The excitation probability $\mathrm{P_e}$ is linked to the probability $\mathrm{P_d}$ of detecting an event in time bin width $\Delta\,\mathrm{t}$ per trigger as

$$\mathrm{P_d} = \frac{\mathrm{N_{d,i}}}{\mathrm{N_T}} = \mathrm{P_e}\Gamma\,\Delta\mathrm{t}\,\eta_r \frac{3\Lambda}{8\pi} \qquad (9)$$

where $\mathrm{P_e}\Gamma$ is the rate at which the atom scatters photons outside the, η_r stays for the losses in APD 1 arm and $\frac{3\Lambda}{8\pi}$ is the fraction of the solid angle subtended by the detection mode. In our setup, η_r was measured to be $\eta_r = 0.3 \pm 0.02$ and $\Lambda = 0.027 \cdot \frac{8\pi}{3}$. By linking the atomic properties to the detected events, we can now investigate the dependence of the excitation probability on number of photons in a pulse and its temporal bandwidth and shape. For example, if we are interested in the probability that the atom is transferred into the excited state by the pulse with certain properties, we can extract the $\mathrm{P_{e,max}}$ from fluorescence histograms. In Figure 5 we show the results of such an experiment, where the maximal excitation probability is plotted with respect to the average photon number in the pulse for different bandwidths.

One sees, that as the bandwidth of the pulse increase, it takes more photons to transfer the atom to the excited state. It is not surprising, since the temporal/frequency overlap is decreasing, the pulse resemble more and more a cw light to the atom. For smaller bandwidths, it is also expected that the overlap should decrease, since frequency bandwidth of the pulse becomes broader then naturally broadened transition bandwidth, but it is not noticeable in our data. More shorter pulses would be needed. To see if there is any benefits in exploiting pulses with different shape, one can ask if there exists an optimal bandwidth for excitation of a two-level atom. Then one can prepare the pulses with this bandwidth and check the excitation probability for same photon number in exponential or square pulse. But from equation 5 one can see, that the coupling strength for a pulse in a coherent state is dependent both on the envelope shape and the number of photons. Thus, the question of the optimum pulse shape rules out — one can always increase photon number to get different coupling. It is however not true for the pulse being in Fock state, since the dependence on N is not present in determination of coupling strenght [**?**]. For the perfect spatial overlap $\Lambda = 8\pi/3$ and Fock state with N=1, the exponential pulse leads to $\mathrm{P_e} = 0.995$, while the rectangular shape gives only $\mathrm{P_e} = 0.81$ [**?**]. But even if there is now good way to de-

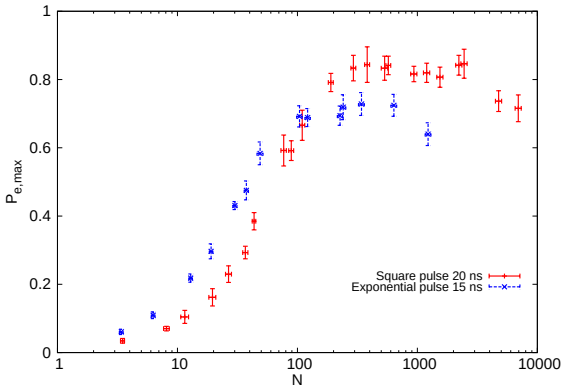

FIG. 6: Maximum excitation probability versus the average photon number for different pulse shapes.

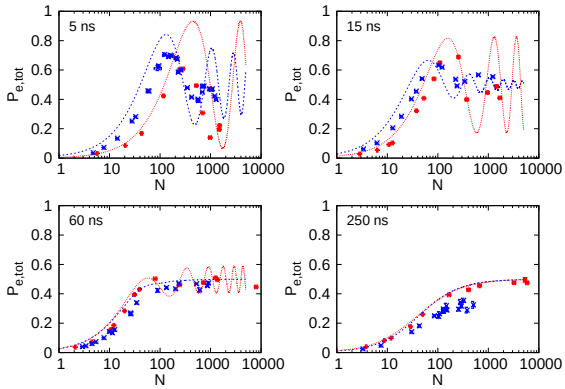

FIG. 7: Total excitation probability versus the average photon number in the pulse. Four plots correspond to different temporal bandwidths.

fine the optimum bandwidth, one still expects the exponential coherent pulse to perform better then rectangular. The figure of merit can be the number of photons required to reach the maximal $\mathrm{P_e}$ for pulses with similar bandwidths but different shapes. The results are shown in Figure 6

One sees, that by using exponential pulse, the excitation probability reaches maximum using less photons then in the rectangular pulse. This results supports the idea that temporal shaping of photons is important for excitation of atoms. In our experiment the difference is not so obvious, but it is expected to become more significant if one uses pulses prepared in Fock states and also by using larger spatial overlap with atomic dipolar emission pattern.

However by focusing on $\mathrm{P_{e,max}}$ we do not see the dynamics of population transfer with increase of N. To observe it, we need to determine the overall excitation probability $\mathrm{P_{e,tot}}$ by pulses with different N. That is, we are interested in what is the probability to find the atom in the excited state right after we switch off the pulse, or what is $\mathrm{P_e}$ at $\Gamma\, t\, =\, 0$ (see Fig 4)? But since our pulses are not perfect, they do not switch off sharply and this quantity is not well defined in our histograms. This value however defines the integral number of counts that one obtains during the exponential decay of atomic population which is governed by $\mathrm{P_e(t)\, =\, \exp(-t\Gamma)}$. Thus taking a probability density function as $-\dot{\mathrm{P}}_\mathrm{e}(\mathrm{t})$ we get **I know it is a bit rough... do we elaborate further on the derivation???**

$$\mathrm{P_{e,tot}\, =\, \frac{\sum_{t\Gamma=0}^{\infty} P_d}{\frac{3\Lambda}{8\pi}\eta\Delta\, t}} \qquad (10)$$

In Figure 7 we show the value of $\mathrm{P_{e,tot}}$ obtained for different bandwidths of the pulses.

The dependence of $\mathrm{P_{e,tot}}$ on N is quite strong for pulses with smaller bandwidth. The duration of the pulses is much less than spontaneous decay time, so the atomic population have less time to decohere. Few Rabi cycles can happen during the time of the pulse, so that the value of $\mathrm{P_{e,tot}}$ may differ dramatically for each N. For larger bandwidths pulses, it takes more photons to form a π-pulse, so the population in the excited state grows more steadily with increase of N.

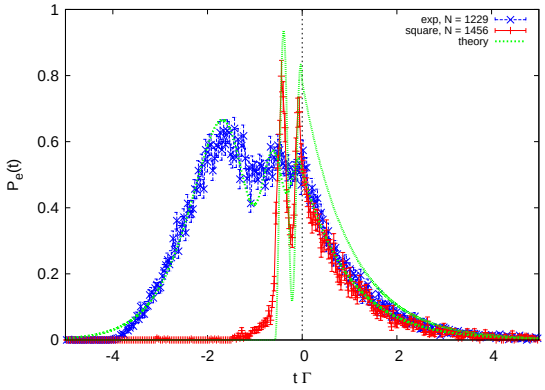

FIG. 8: Excitation probability versus the time. Rabi oscillations are clearly visible.

In order to use atom-photon interface as a basis for optical switching, it is important to ensure that the atomic response is nonlinear with respect to incoming field. Numerous experiments with atoms and solid state systems in cavities demonstrated that nonlinear behaviour of atom+cavity system can be observed for extremely low ($\mathrm{N} \ll 1$) photon number. In the abscence of cavities it was also shown that single dye molecules can be used as an optical switch for $\mathrm{N} \approx 500$ [**?**]. In these experiments the observation of Rabi oscillations manifests the ability of switching. When the atom is transferred to excited state by a pulse (maximum of Rabi flops), it becomes transparrent for the subsequent pulse that is sent to it. When the atomic population is in the ground state, the second pulse have a high chance to be absorbed. In Figure 8 we show the coherent dynamics of atomic population by using pulses of 15 ns bandwidth with $\mathrm{N} \approx 1300$

CONCLUSION

We have investigated the interaction of temporaly shaped pulses with a single trapped atom. We demonstrated that the atomic population can be transferred to the excited state with high probability with relatively low photon number coherent pulse. It was shown, that the excitation of the atom is sensitive to the envelope of the excitation pulse; the rising exponential pulse performs better than the rectangular. Rabi oscillations of a single atom were observed for ≈ 1000 photons in a pulse. This shows the feasibility of using a single atom as a switch for pulses with low photon number. Nevertheless, the spatial overlap of pulse mode and atomic emission mode should be significantly enhanced to observe interaction between two ligth pulses at single photon level. The possibility of using Fock states instead of weak coherent pulses is also advantageous, since all the effects observed in this letter should be more profound.

ACKNOWLEDGMENT

We acknowledge the support of this work by the National Research Foundation & Ministry of Education in Singapore.

* Center for Quantum Technologies 3 Science Drive 2, Singapore, 117543
† University of Twente
‡ Center for Quantum Technologies and Department of Physics, National University of Singapore, 3 Science Drive 2, Singapore, 117543; christian.kurtsiefer@gmail.com

[1] J. I. Cirac, P. Zoller, H. J. Kimble, and H. Mabuchi, Phys. Rev. Lett. **78**, 3221 (1997).
[2] L.-M. Duan, M. D. Lukin, J. I. Cirac, and P. Zoller, Nature **414**, 413 (2001).
[3] P. W. H. Pinkse, T. Fischer, P. Maunz, and G. Rempe, Nature 365 **404** (2000).
[4] A. D. Boozer, A. Boca, R. Miller, T. E. Northup, and H. J. Kimble, Phys. Rev. Lett. **98**, 193601 (2007).
[5] M. K. Tey, G. Maslennikov, T. C. H. Liew, S. A. Aljunid, F. Huber, B. Chng, Z. Chen, V. Scarani, and C. Kurtsiefer, New J. Phys. **11**, 043011 (2009).
[6] G. Zumofen, N. M. Mojarad, V. Sandoghdar, and M. Agio, Phys. Rev. Lett. **101**, 180404 (2008).
[7] A. N. Vamivakas, M. Atature, J. Dreiser, S. T. Yilmaz, A. Badolato, A. K. Swan, B. B. Goldberg, A. Imamoglu, and M. S. Unlu, Nano Letters **7**, 2892 (2007).
[8] G. Wrigge, I. Gerhardt, J. Hwang, G. Zumofen, and V. Sangoghdar, Nature Physics **4**, 60 (2008).
[9] M. K. Tey, Z. Chen, S. A. Aljunid, B. Chng, F. Huber, G. Maslennikov, and C. Kurtsiefer, Nature Physics **4**, 924 (2008).
[10] C. M. Savage, S. L. Braunstein, and D. F. Walls, Opt. Lett. **15**, 628 (1990).
[11] Q. A. Turchette, C. J. Hood, W. Lange, H. Mabuchi, and H. J. Kimble, Phys. Rev. Lett. **75**, 4710 (1995).
[12] I. Fushman, D. Englund, A. Faraon, N. Stoltz, P. Petroff, and J. Vuckovic, Science **320**, 769 (2008).
[13] A. S. Zibrov, M. D. Lukin, L. Hollberg, D. E. Nikonov, M. O. Scully, H. G. Robinson, and V. L. Velichansky, Phys. Rev. Lett. **76**, 3935 (1996).
[14] G. Zumofen, N. Mojarad, and M. Agio, Nuovo Cimento C **31**, 475 (2009).
[15] N. Schlosser, G. Reymond, and P. Grangier, Phys. Rev. Lett. **89**, 023005 (2002).
[16] R. Juskaitis and T. Wilson, Journal of Microscopy **189**, 8 (1997).
[17] S. Quabis, R. Dorn, M. Eberler, G. O., and G. Leuchs, Applied Physics B **72**, 109 (2001).
[18] S. K. Rhodes, K. A. Nugent, and A. Roberts, J. Opt. Soc. Am. A **19**, 1689 (2002).
[19] M. Weber, J. Volz, K. Saucke, C. Kurtsiefer, and H. Weinfurter, Physical Review A **73**, 043406 (2006).
[20] C. Tuchendler, A. M. Lance, A. Browaeys, Y. R. P. Sortais, and P. Grangier, Physical Review A **78**, 033425 (2008).
[21] M. Kasevich and S. Chu, Phys. Rev. Lett. **69**, 1741 (1992).
[22] H. J. Lee, C. S. Adams, M. Kasevich, and S. Chu, Phys. Rev. Lett. **76**, 2658 (1996).